



Realizing Efficient Wireless Power Transfer in the Near-Field Region Using Electrically Small Antennas

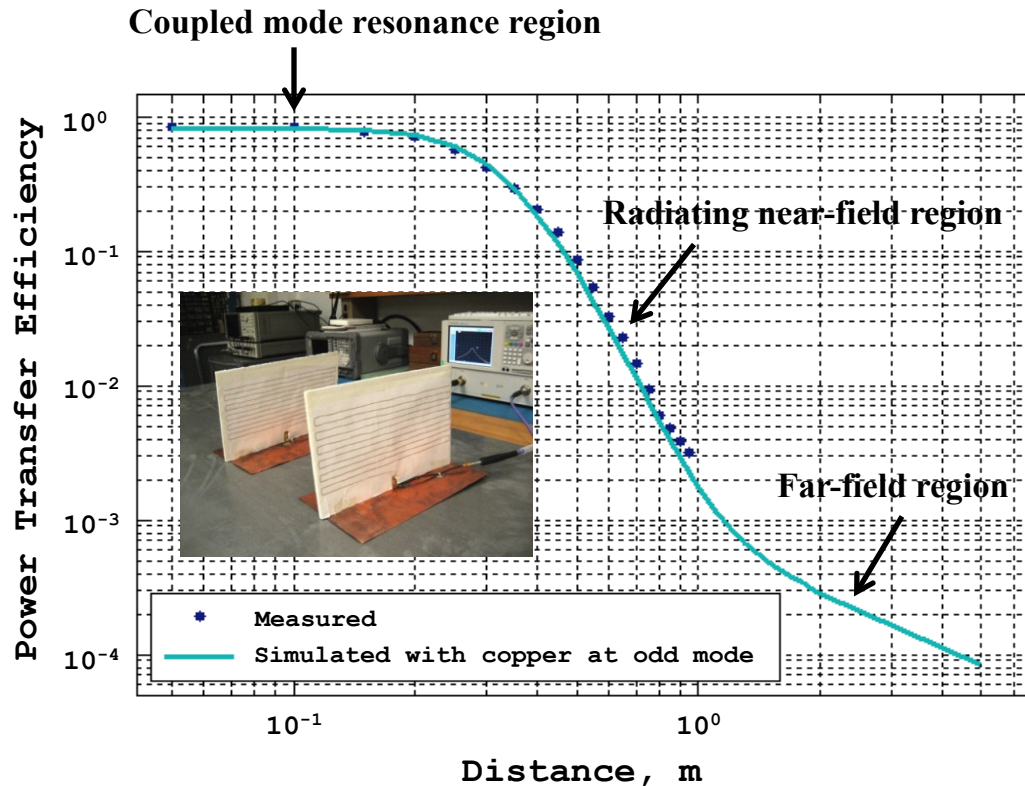
Ick-Jae Yoon¹ and Hao Ling²

¹Dept. of Electrical Engineering, Technical University of Denmark

²Dept. of Electrical and Computer Engineering, University of Texas at Austin

yoona@elektro.dtu.dk

- Potential applications of near-field wireless power transfer
 - Powering or charging of handheld devices, electric vehicles, autonomous robots, implanted devices and unattended sensors
- Two distinct regions of interest for near-field wireless power transfer



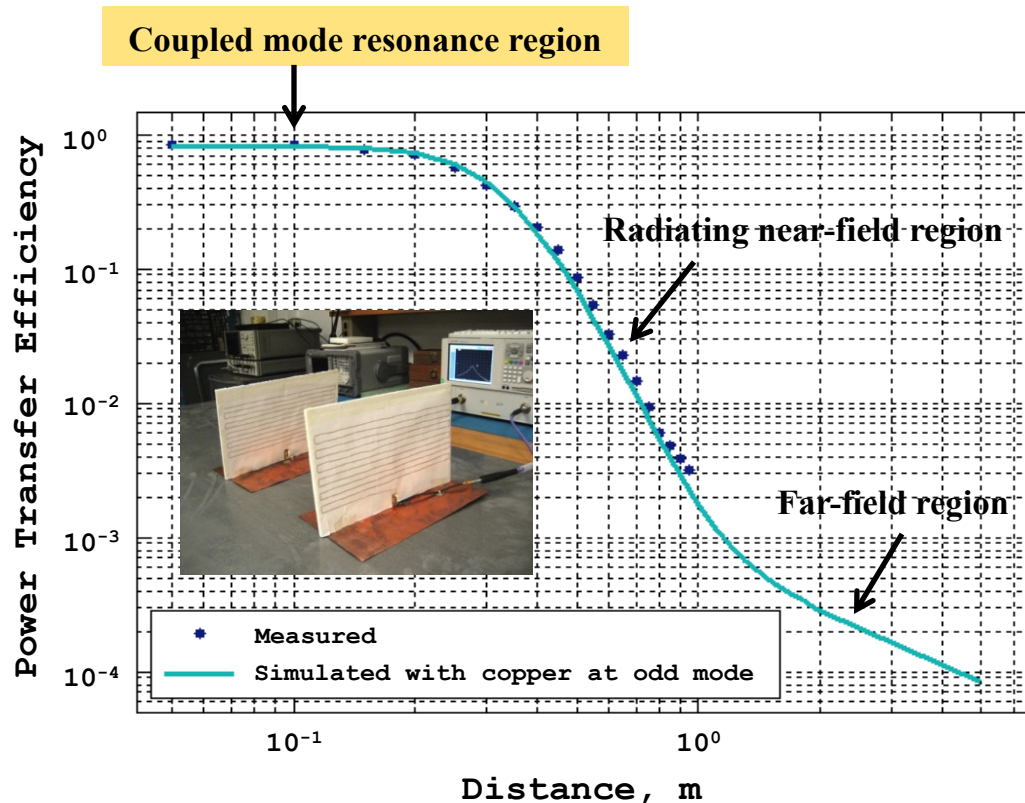
Coupled mode resonance region

- Very close range
- High power transfer efficiency (PTE)
- Frequency splitting phenomenon
- Impedance matching is challenging
- Physics is complex (coupled mode theory)

Radiating near-field region

- Efficiency drops rapidly
- But longer range possible
- Physics derived using spherical wave theory
- Impedance matching is not difficult
- Efficient antenna design is key

- Potential applications of near-field wireless power transfer
 - Powering or charging of handheld devices, electric vehicles, autonomous robots, implanted devices and unattended sensors
- Two distinct regions of interest for near-field wireless power transfer



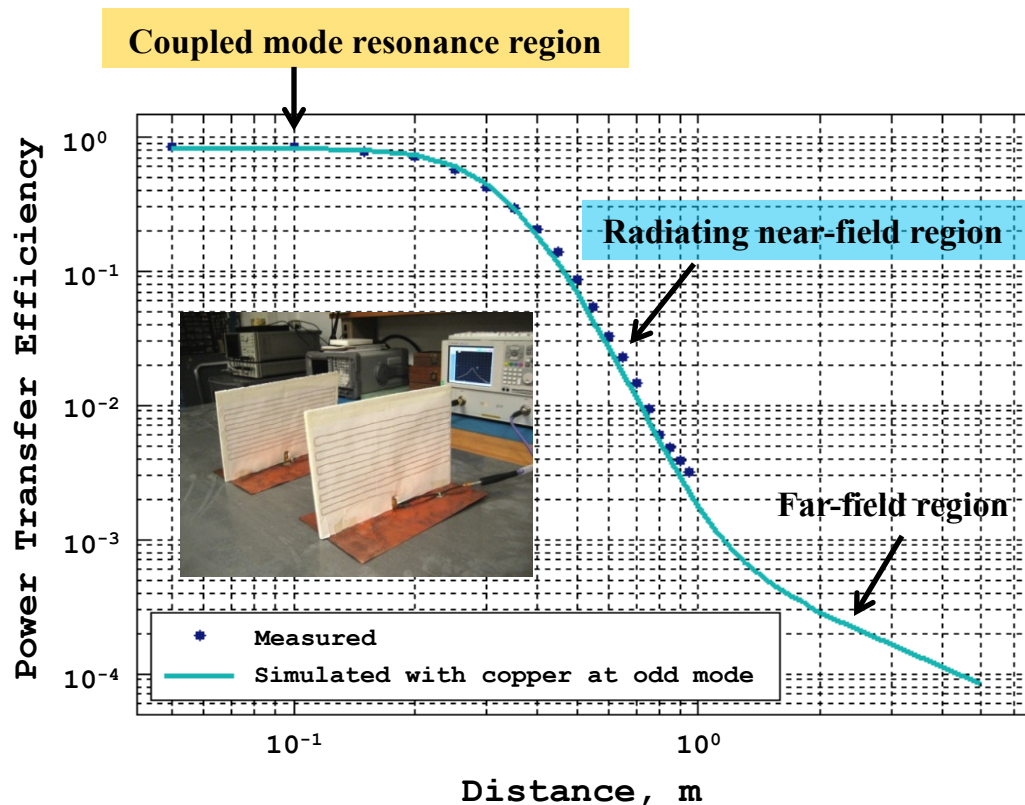
Coupled mode resonance region

- Very close range
- High power transfer efficiency (PTE)
- Frequency splitting phenomenon
- Impedance matching is challenging
- Physics is complex (coupled mode theory)

Radiating near-field region

- Efficiency drops rapidly
- But longer range possible
- Physics derived using spherical wave theory
- Impedance matching is not difficult
- Efficient antenna design is key

- Potential applications of near-field wireless power transfer
 - Powering or charging of handheld devices, electric vehicles, autonomous robots, implanted devices and unattended sensors
- Two distinct regions of interest for near-field wireless power transfer



Coupled mode resonance region

- Very close range
- High power transfer efficiency (PTE)
- Frequency splitting phenomenon
- Impedance matching is challenging
- Physics is complex (coupled mode theory)

Radiating near-field region

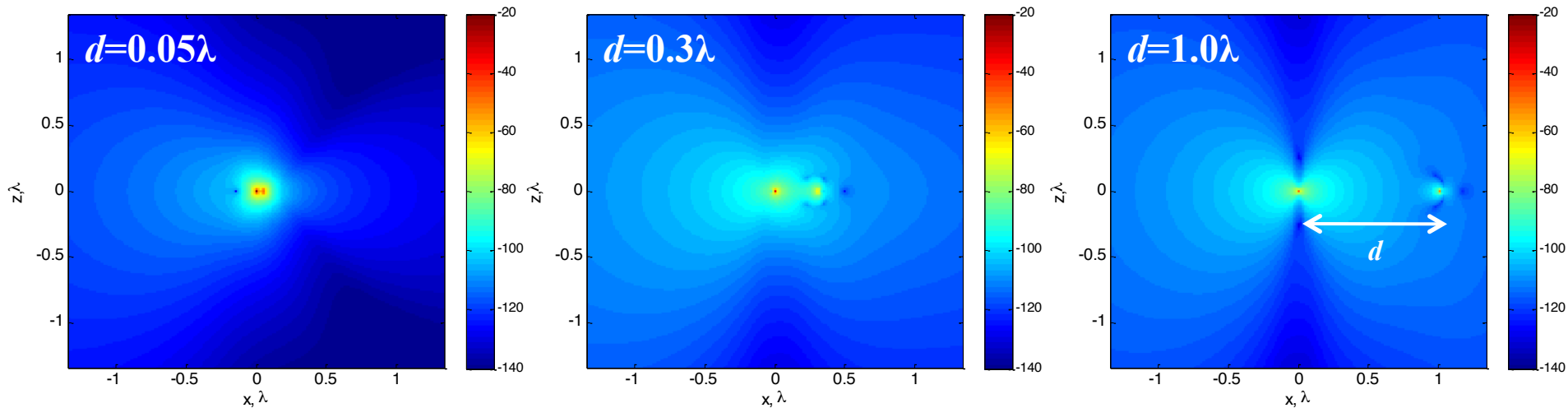
- Efficiency drops rapidly
- But longer range possible
- Physics derived using spherical wave theory
- Impedance matching is not difficult
- Efficient antenna design is key

- Power flow between antennas in different regions
 - Real part of Poynting vector plot (in dB) with two short dipoles (Tx-Rx, $\lambda/50$)
 - d : distance between the antennas

|| *Coupled mode region* ||

|| *Radiating near-field region* ||

|| *Far-field region* ||



Realizing efficient wireless power transfer *in the radiating near-field region* using electrically small antennas

- Objectives and Outline

Objective 1: Achieving theoretical power transfer efficiency bound using electrically small antennas

Objective 2: Wireless power transfer enhancement using transmitter diversity and receiver diversity

Objective 3: Investigation of near-field wireless power transfer in the presence of lossy dielectric materials

Objective 4: Power transfer enhancement using small directive antennas

Objective 5: Alleviating orientation dependence in near-field wireless power transfer using small, circular polarization antennas

Realizing efficient wireless power transfer *in the radiating near-field region* using electrically small antennas

- Objectives and Outline

Objective 1: Achieving theoretical power transfer efficiency bound using electrically small antennas

Objective 2: Wireless power transfer enhancement using transmitter diversity and receiver diversity

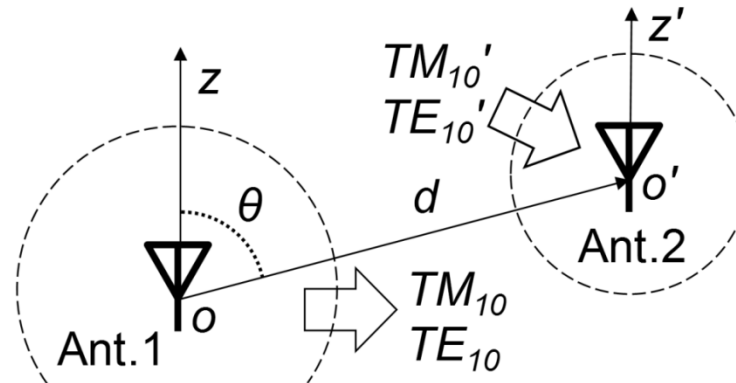
Objective 3: Investigation of near-field wireless power transfer in the presence of lossy dielectric materials

Objective 4: Power transfer enhancement using small directive antennas

Objective 5: Alleviating orientation dependence in near-field wireless power transfer using small, circular polarization antennas

Objective 1: Achieving theoretical power transfer efficiency bound using electrically small antennas

- Theoretical PTE bound by the spherical mode theory for small antennas
[Lee and Nam, *IEEE AP Trans.*, 2010]

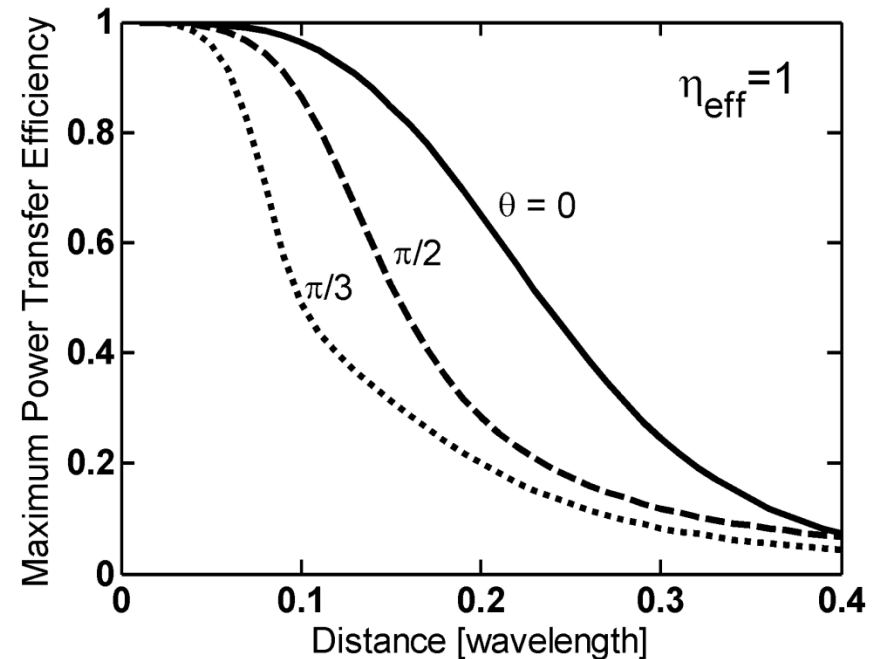
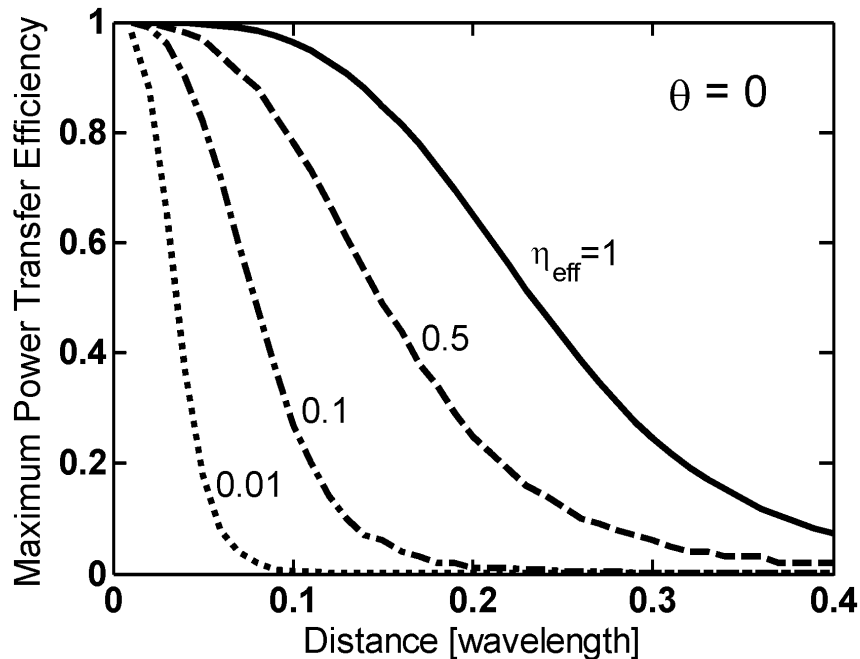


- Only the lowest TE_{10} and TM_{10} modes are assumed.
- Optimal load for max. power transfer is assumed.
- Describe the coupling network between two antennas as Z-parameter.

$$- PTE^{max} = \frac{|X|^2}{2 - Re[X^2] + \sqrt{4(1 - Re[X^2]) - Im[X^2]^2}}$$

$$X = \eta \times \frac{3}{2} \left[-\sin^2 \theta \frac{1}{jkd} + (3 \cos^2 \theta - 1) \times \left\{ \frac{1}{(jkd)^2} + \frac{1}{(jkd)^3} \right\} \right] e^{-jkd}$$

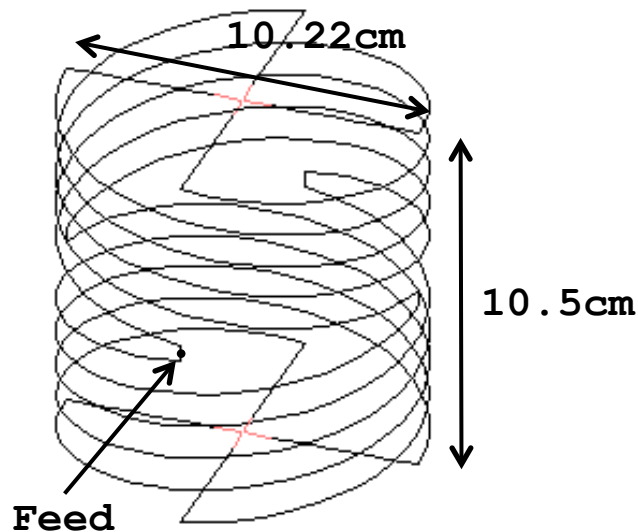
- Theoretical results – dependence on efficiency and orientation



- *PTE* increases as the radiation efficiency η_{eff} increases
 - Efficient, electrically small antennas
- Up to a distance of 0.4λ , higher PTE is achieved when the two antennas are co-linear ($\theta=0$) than when they are in the parallel configuration ($\theta=\pi/2$).

2. Antenna design

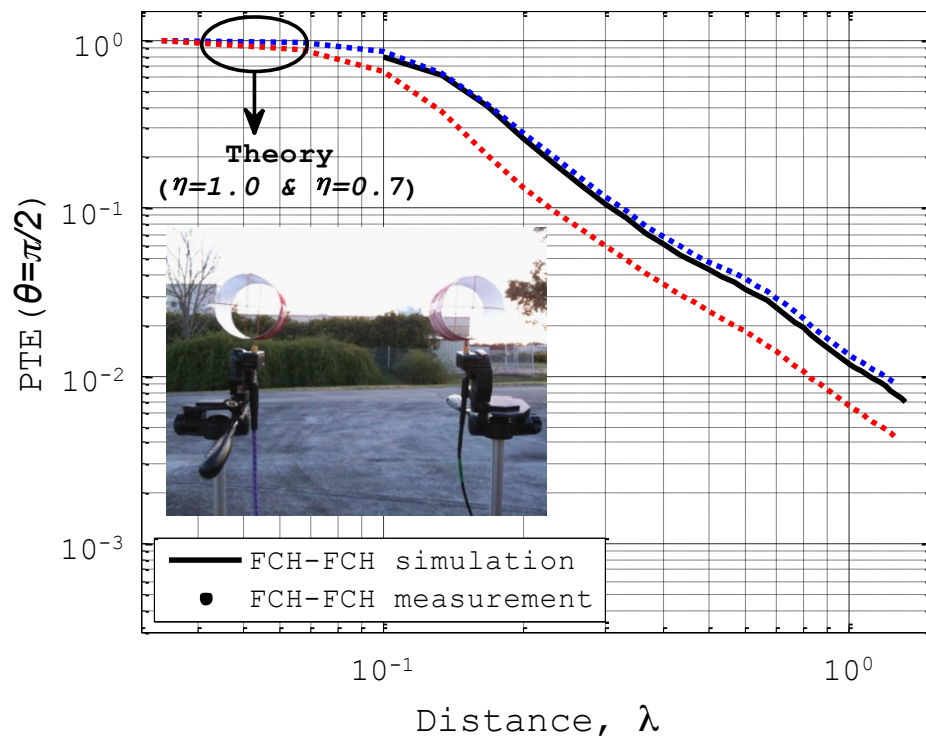
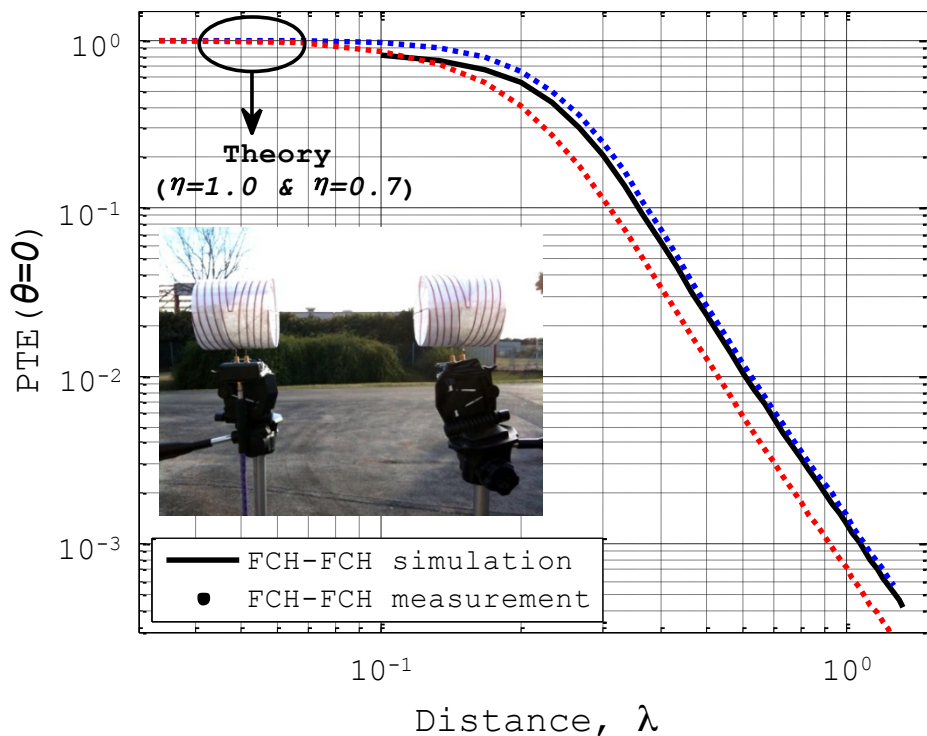
- Design of folded cylindrical helix (FCH) dipole
 - $kr=0.31$; Radiation efficiency=93%; Input impedance=49 Ω ; $f_o = 200$ MHz
 - Two FCHs are built for transmitting and receiving. Made of copper.
 - Each feed point is connected to a balun.



	Sim.	Meas. (Tx FCH)	Meas. (Rx FCH)
f_o	200.0MHz	195.0MHz	194.8MHz
R_{in}	48.89 Ω	49.07 Ω	48.92 Ω

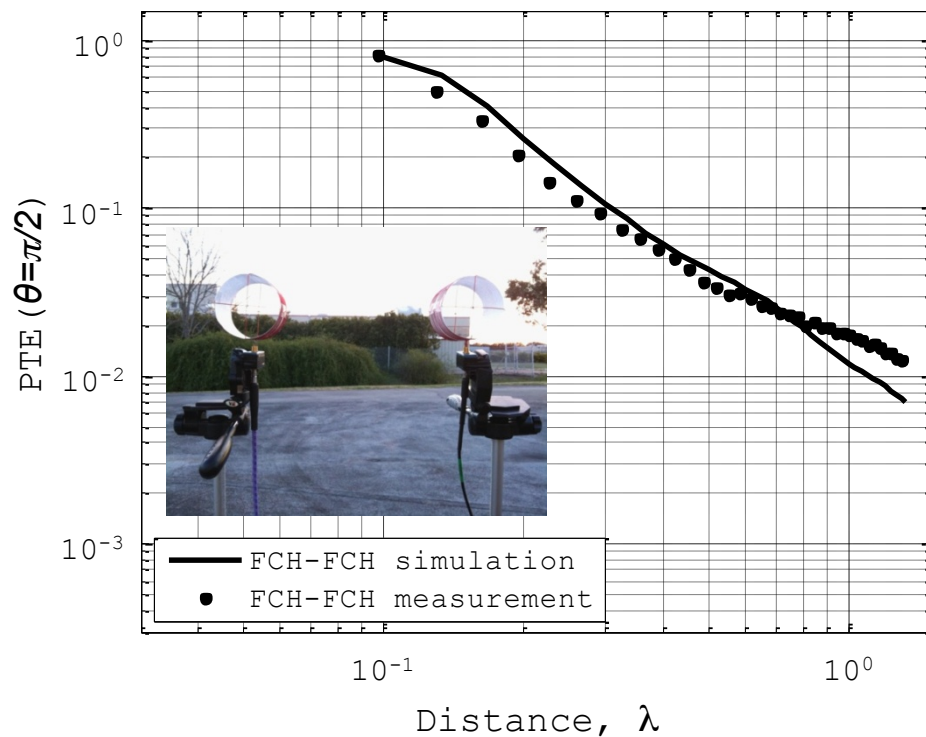
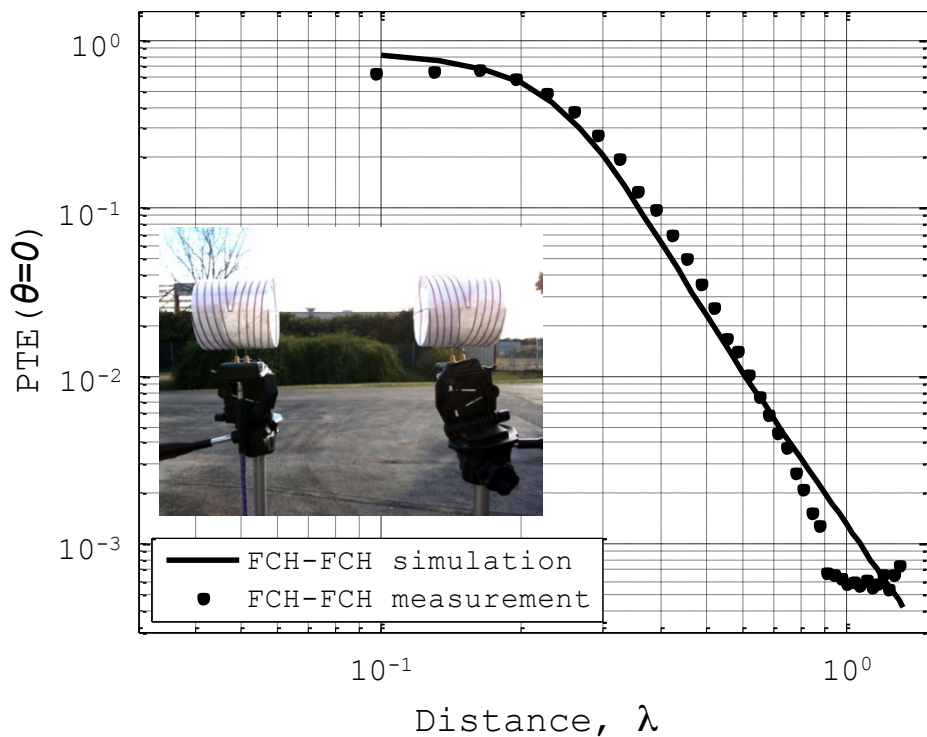
3. PTE of FCH-FCH dipole coupling

- PTE measurement using the two designed FCH dipoles
 - Measurement using vector network analyzer
 - $PTE = |S_{21}|^2 / (1 - |S_{11}|^2)$
 - 50-Ω load in Rx FCH in NEC simulation
 - PTE of 40% is achieved at a distance of 0.25λ (0.39m at 195MHz)
 - Very close to the theoretical bound: 42.6% at 0.25λ



3. PTE of FCH-FCH dipole coupling

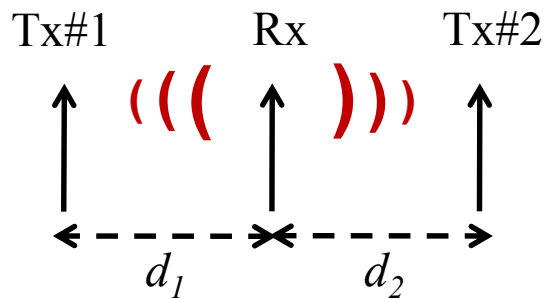
- PTE measurement using the two designed FCH dipoles
 - Measurement using vector network analyzer
 - $PTE = |S_{21}|^2 / (1 - |S_{11}|^2)$
 - 50-Ω load in Rx FCH in NEC simulation
 - PTE of 40% is achieved at a distance of 0.25λ (0.39m at 195MHz)
 - Very close to the theoretical bound: 42.6% at 0.25λ



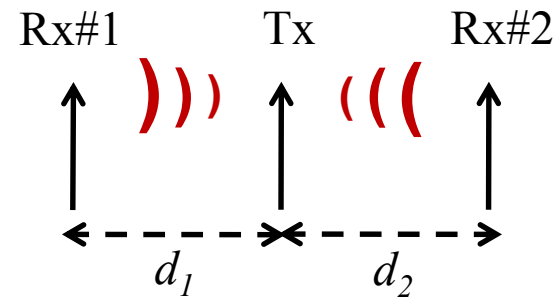
- Review of the theoretical PTE bound
 - Derived previously by Lee and Nam using the spherical mode theory
 - Verification of the theory by short dipoles coupling simulation
- Practical antenna design considerations
 - Highly efficient small antenna with 50Ω input impedance
- Antenna design and measurement
 - Folded Cylindrical Helix (FCH) dipole antenna: ($kr=0.31$, $R_{in}=50\Omega$ & $\eta=0.93$)
- PTE simulation and measurement
 - For both co-linear ($\theta=0$) and parallel configurations ($\theta=\pi/2$)
 - Measurement result: a PTE of 40% at a distance of 0.25λ in the co-linear configuration, very close to the theoretical bound (42.6% at 0.25λ)

I.-J. Yoon and H. Ling, "Realizing efficient wireless power transfer using small folded cylindrical helix dipoles," *IEEE Antennas and Wireless Propag. Lett.*, vol. 9, pp. 846–849, 2010.

Objective 2: Wireless power transfer enhancement using transmitter diversity and receiver diversity



Transmitter diversity
($d_1 + d_2 = \text{const.}$)



Receiver diversity
($d_1 = d_2$)

- PTE definition for multiple transmitters (Tx) and a single receiver (Rx)

$$- PTE = \frac{\text{Power dissipated in the load}}{\sum \text{Power accepted by transmit antennas}} = \frac{\text{Re}\{Z_{load}\} \cdot |I_3|^2 / 2}{\text{Re}\{V_1 \cdot I_1^*\} / 2 + \text{Re}\{V_2 \cdot I_2^*\} / 2}$$

- Port 3: receiver, Port 1 & 2: transmitters

- Terminal currents

- With input voltages specified at the Tx ports and a given load, the terminal currents can be obtained once the 3-by-3 Z-matrix of the network is known:

$$\begin{bmatrix} Z_{11} & Z_{12} & Z_{13} \\ Z_{21} & Z_{22} & Z_{23} \\ Z_{31} & Z_{32} & Z_{33} \end{bmatrix} \begin{bmatrix} I_1 \\ I_2 \\ I_3 \end{bmatrix} = \begin{bmatrix} V_1 \\ V_2 \\ -I_3 \cdot Z_{load} \end{bmatrix}$$

- Z_{load}

- Need to find optimal load (Z_{opt}) for maximum coupling among the antennas

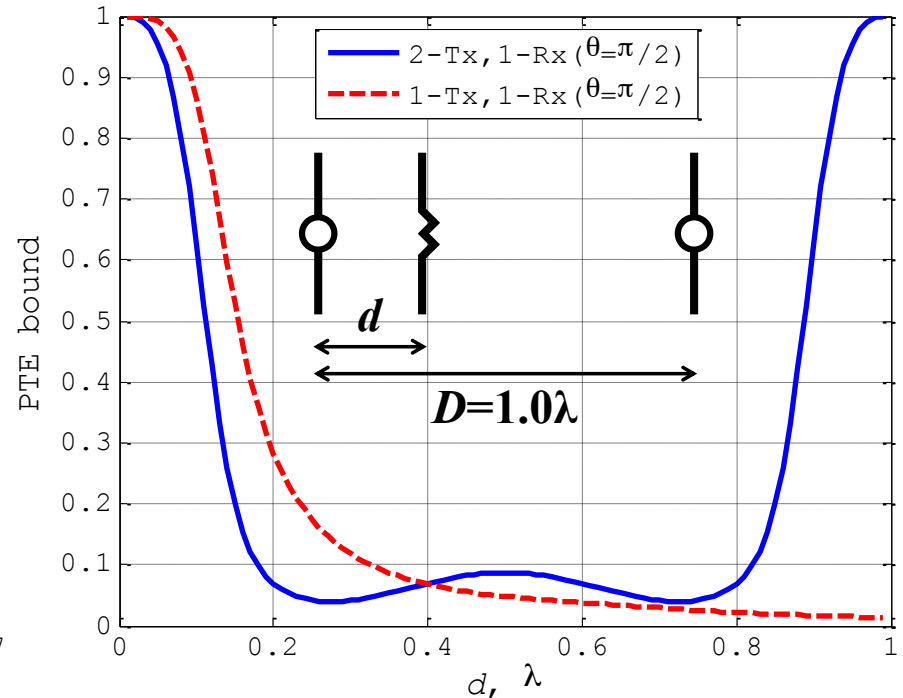
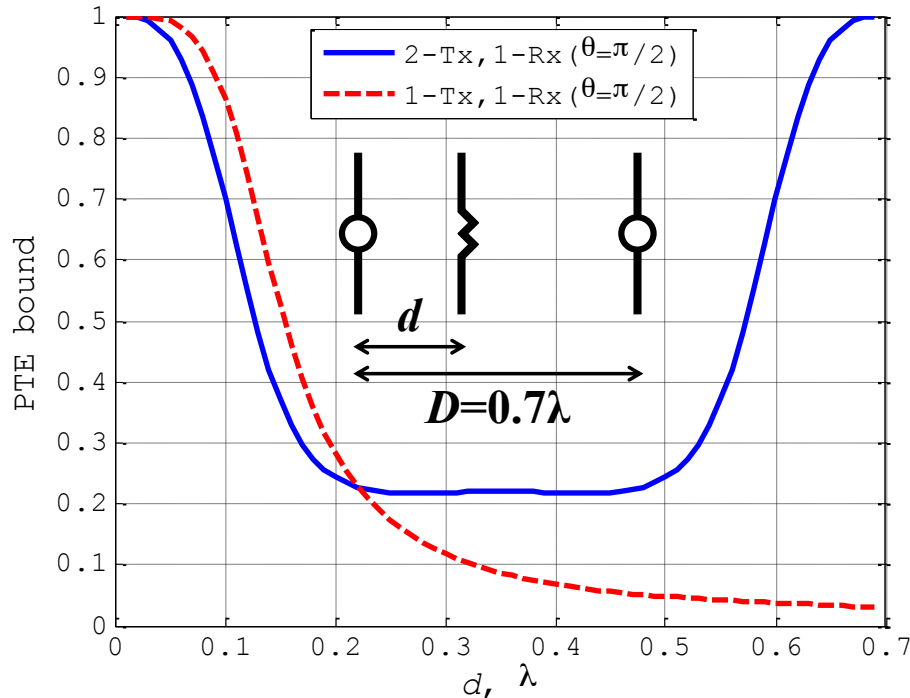
- For calculating Z -matrix
 - Extending the mutual impedance expression between two electrically small dipole antennas derived by Lee and Nam to the multiport case.

$$Z_{mn} = \begin{cases} Z_a, & m = n \\ \text{Re}[Z_a] \cdot T, & m \neq n \end{cases}$$

$$T = 1.5 \cdot \eta \cdot \left[-\sin^2 \theta \frac{1}{jkd} + (3 \cos^2 \theta - 1) \cdot \left\{ \frac{1}{(jkd)^2} + \frac{1}{(jkd)^3} \right\} \right] \cdot e^{-jkd}$$

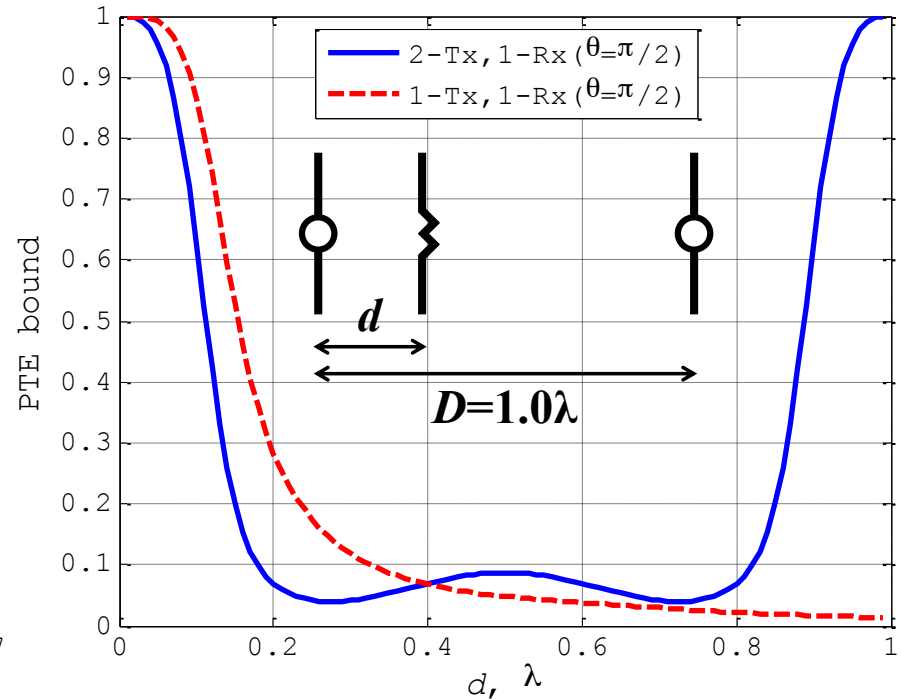
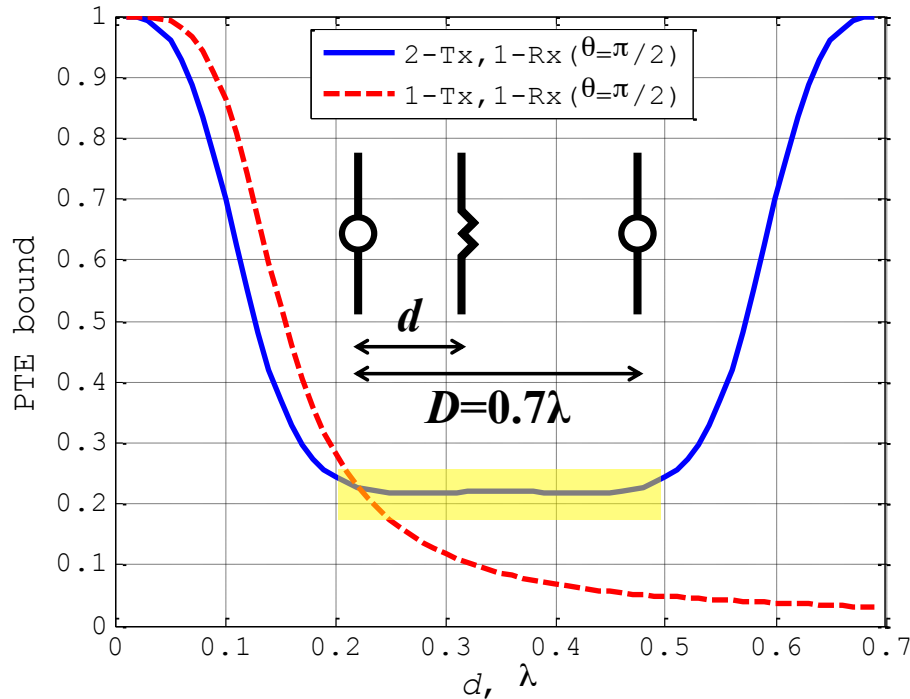
- Z_a = stand-alone input impedance of a small dipole
-
- For calculating Z_{opt}
 - Linville method is NOT valid for this problem.
 - It's only good for 2-port network.
 - Local optimizer can be used instead.
 - Initial seed = $Z_{a, Rx}^*$

- A receiver between two transmitters in the parallel configuration ($\theta=\pi/2$)



- Very stable PTE region as a function of receiver position is created for $D=0.7\lambda$.
 - 22% of PTE over 0.2λ - 0.5λ region
- Ripples start to appear in the PTE curve at larger spacings ($D=1.0\lambda$)
 - Standing wave interference between the fields from two transmitters

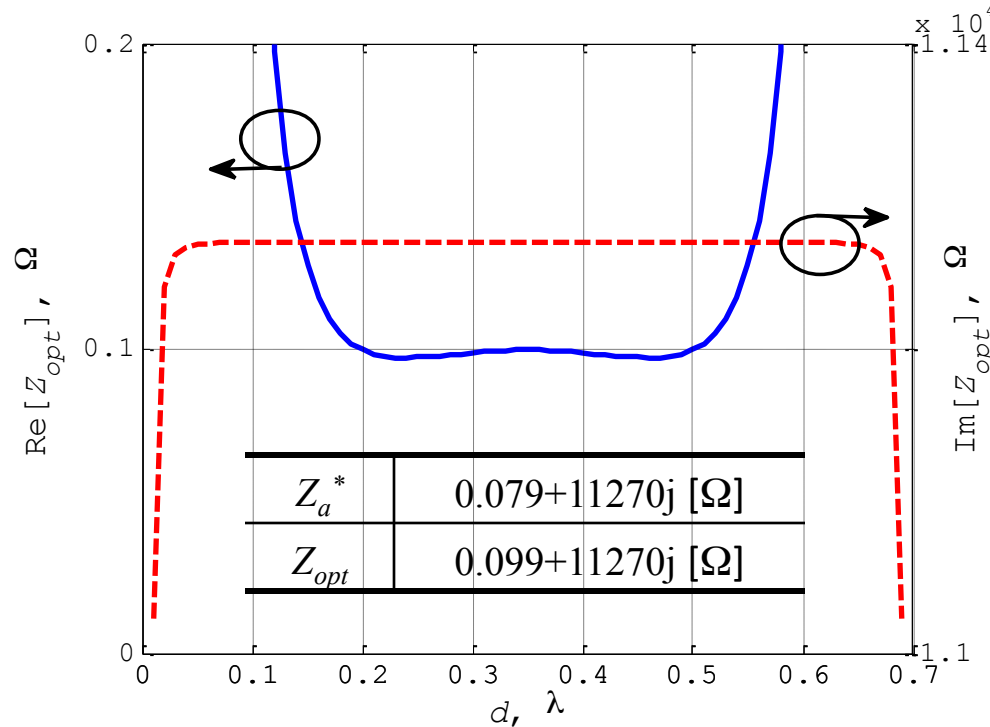
- A receiver between two transmitters in the parallel configuration ($\theta=\pi/2$)



- Very stable PTE region as a function of receiver position is created for $D=0.7\lambda$.
 - 22% of PTE over 0.2λ - 0.5λ region
- Ripples start to appear in the PTE curve at larger spacings ($D=1.0\lambda$)
 - Standing wave interference between the fields from two transmitters

2. Practical antenna design considerations

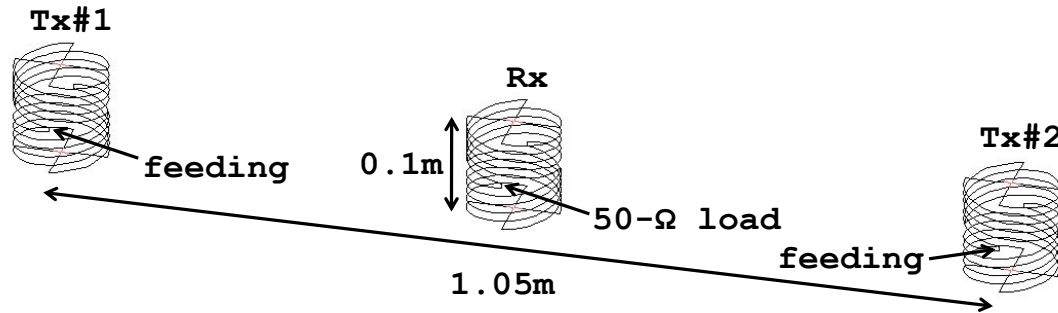
- Z_{opt} for the PTE bound respect to $Z_a = 0.079 - 11270j$ [Ω] ($D = 0.7\lambda$)



- Z_{opt} is also rather stable in the flat PTE region of $0.2\lambda - 0.5\lambda$. In particular, its numerical value is close to the conjugate of the input impedance of the stand-alone antenna. → **50 Ω input impedance for Rx antenna.** (If 50- Ω load is desired.)
- Lower radiation efficiency lowers the PTE significantly. → **Highly efficient antennas**

3. PTE simulation and measurement

- NEC simulation setup
 - Each antenna has input impedance of 48.9Ω and efficiency of 93% at 200MHz.
 - Fixed $50\text{-}\Omega$ load at Rx FCH.



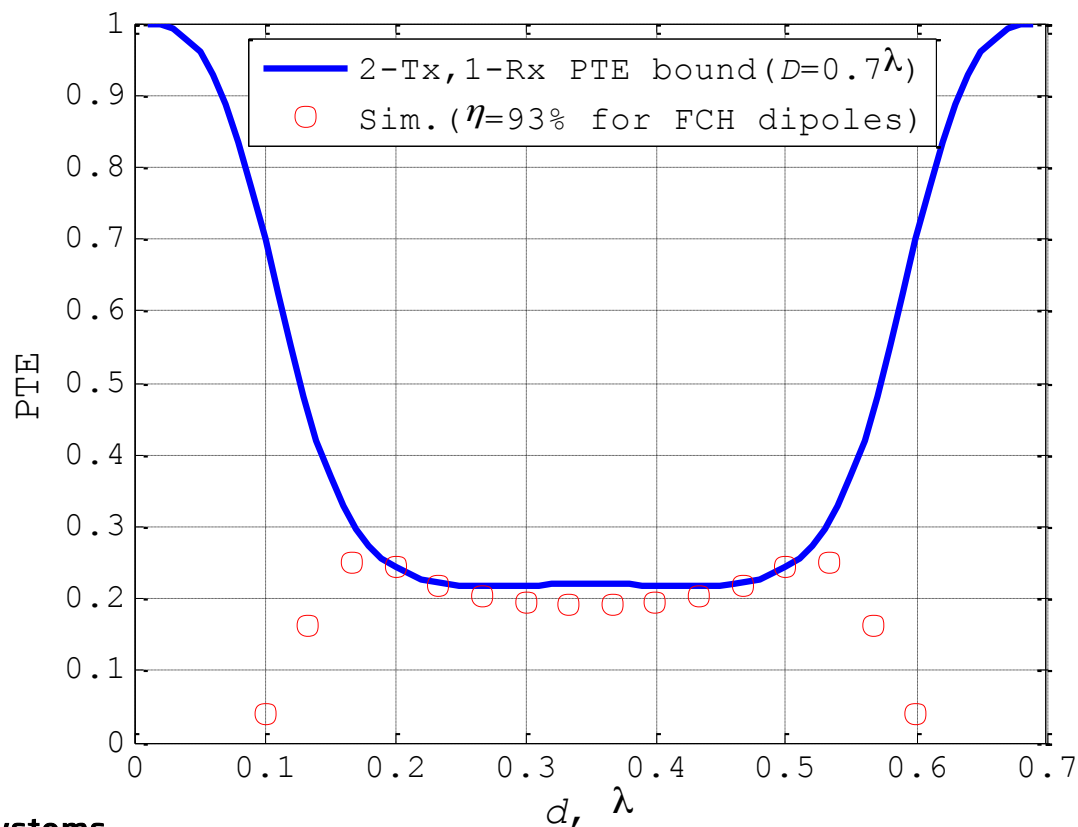
- Measurement setup
 - Three FCH dipoles are fabricated ($f_o=194.5\text{MHz}$).



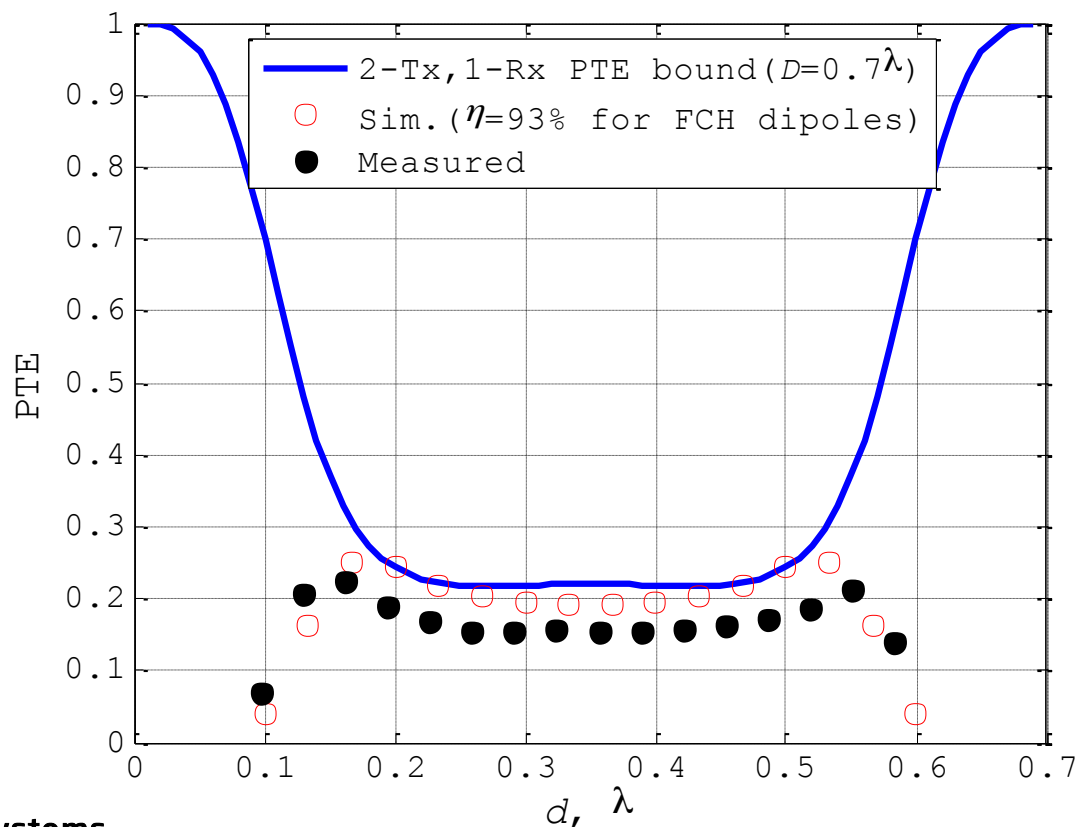
	f_o , MHz	R_{in} , Ω
Tx#1	194.4	61.66
Tx#2	194.5	63.52
Rx	194.5	55.28

$$PTE_{meas} = \frac{|S_{31} + S_{32}|^2}{1 - |S_{11} + S_{12}|^2 + 1 - |S_{22} + S_{21}|^2}$$

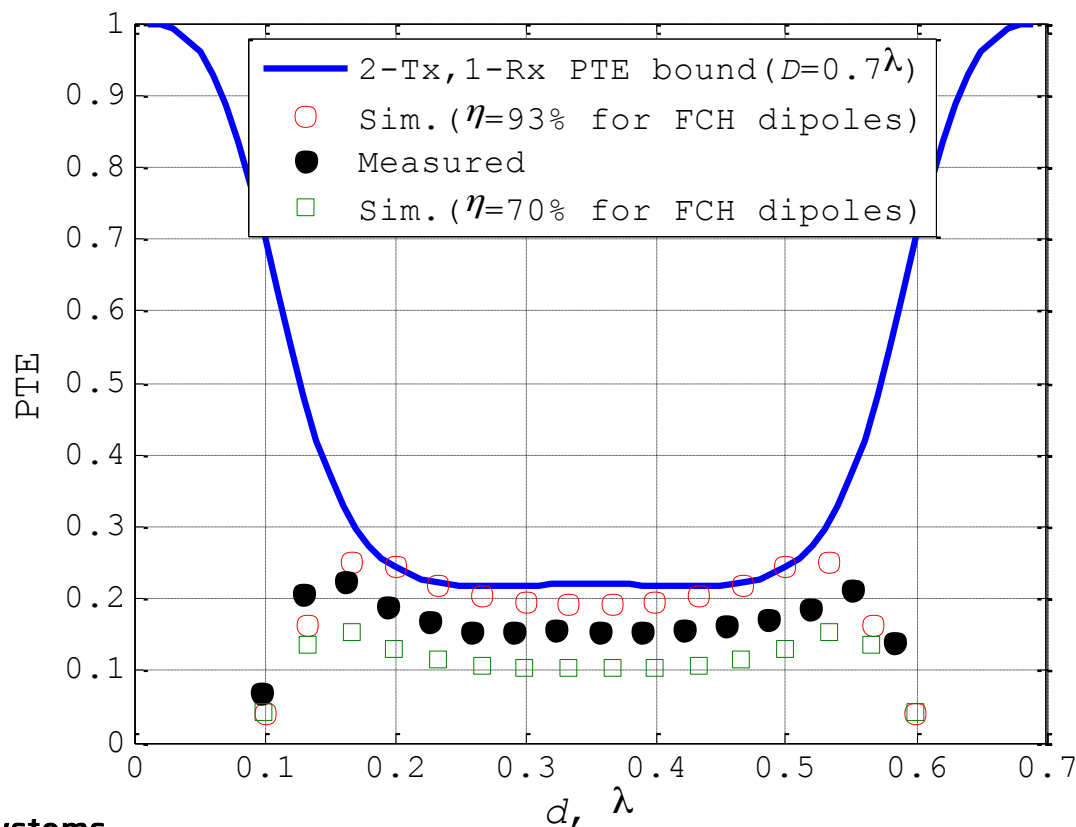
- Simulated and measured PTE ($D=0.7\lambda$)
 - Simulated PTE approaches the theoretical PTE bound showing 20% stable PTE region from 0.2λ to 0.5λ .
 - Measured PTE follows the trend of the simulation, showing the same stable PTE region. Level is about 3% lower than the simulation (17%).



- Simulated and measured PTE ($D=0.7\lambda$)
 - Simulated PTE approaches the theoretical PTE bound showing 20% stable PTE region from 0.2λ to 0.5λ .
 - Measured PTE follows the trend of the simulation, showing the same stable PTE region. Level is about 3% lower than the simulation (17%).



- Simulated and measured PTE ($D=0.7\lambda$)
 - Simulated PTE approaches the theoretical PTE bound showing 20% stable PTE region from 0.2λ to 0.5λ .
 - Measured PTE follows the trend of the simulation, showing the same stable PTE region. Level is about 3% lower than the simulation (17%).

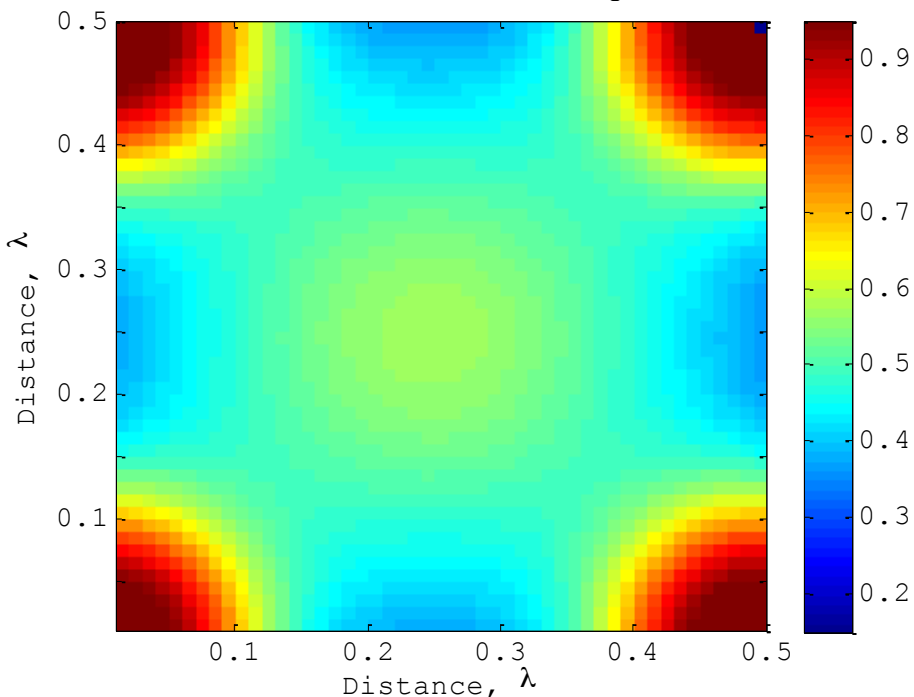


4. Four transmitter and a single receiver

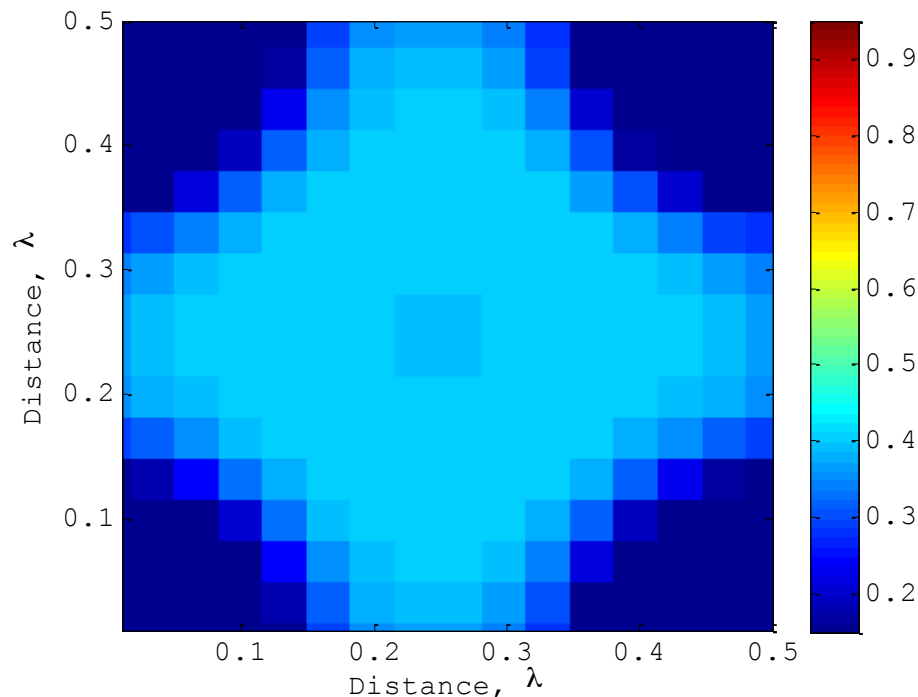
■ PTE bound and NEC simulation

- Four transmitters are located at the corners of a square region. The length of the diagonal line is set to 0.7λ and a single receiver is moved within the region.
- Same formulation is used, except a 5-port network is considered.
- Z_{opt} is found through a numerical search.

|| PTE bound ($Z_L=Z_{opt}$) ||



|| FCH dipoles ($Z_L=50\Omega$) ||



- PTE bound derivation for transmitter diversity and receiver diversity
 - Transmitter diversity: showing a stable PTE region for sufficiently close spacing between two transmitters
 - Receiver diversity: showing a PTE bound extended by the increased number of receivers

- Practical antenna design considerations
 - Highly efficient small antenna with 50Ω input impedance
 - Folded Cylindrical Helix (FCH) dipole antenna: ($kr=0.31$, $R_{in}=50\Omega$ & $\eta=0.93$)

- PTE simulation and measurement (transmitter diversity)
 - Measurement result: a 17% PTE values over a 0.3λ region between the two transmitters, corroborating the theory and simulation.

- Four transmitter case over two-dimensional region
 - The stable PTE region can be extended to two-dimensional space.

I.-J. Yoon and H. Ling, "Investigation of near-field wireless power transfer under multiple transmitters," *IEEE Antennas and Wireless Prostag. Lett.*, vol. 10, pp. 662–665, 2011.

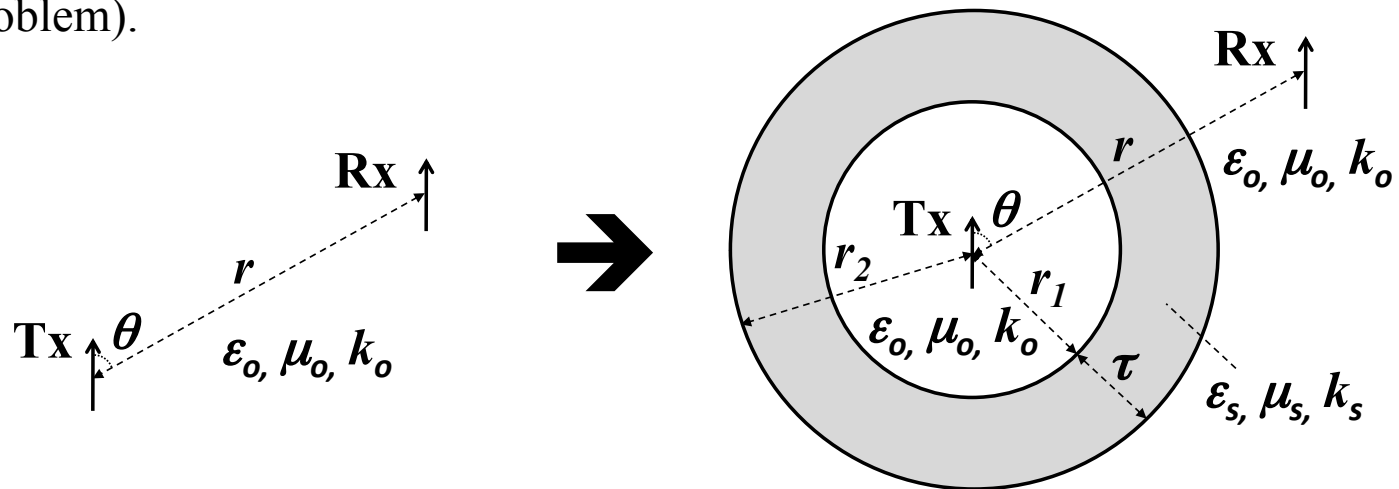
Objective 3: Investigation of near-field wireless power transfer in the presence of lossy dielectric materials

- Near-field wireless power transfer (WPT) in free space has been well characterized.
- The interactions of near fields with materials need to be quantified to address practical deployment issues.
 - WPT works regarding material effects so far → based on numerical simulations and measurements.

Goal and outline of this research:

1. Derive an analytic PTE bound in the radiating near-field region when a small transmit (Tx) antenna is enclosed by a material shell and a small receive (Rx) antenna is located outside in free space. (The shell problem is described in the next page.)
2. Validation of the theory using FEKO simulation.
3. Study material effects on WPT using the derived closed form expression.
4. Through-wall measurement.

- Material shell problem description
 - Starting from Lee & Nam's PTE derivation in free space using spherical mode theory, our derivation considers an additional pair of incoming and outgoing spherical waves within the shell (i.e. we modify PTEfs in accordance with the shell problem).



Assumptions in material shell problem:

- Only the lowest TM_{10} or TE_{10} spherical mode is radiated from the source.
- The scattering from the Tx and Rx antennas is negligible due to their small size.

- The final close-form expression for the TM mode is given by:

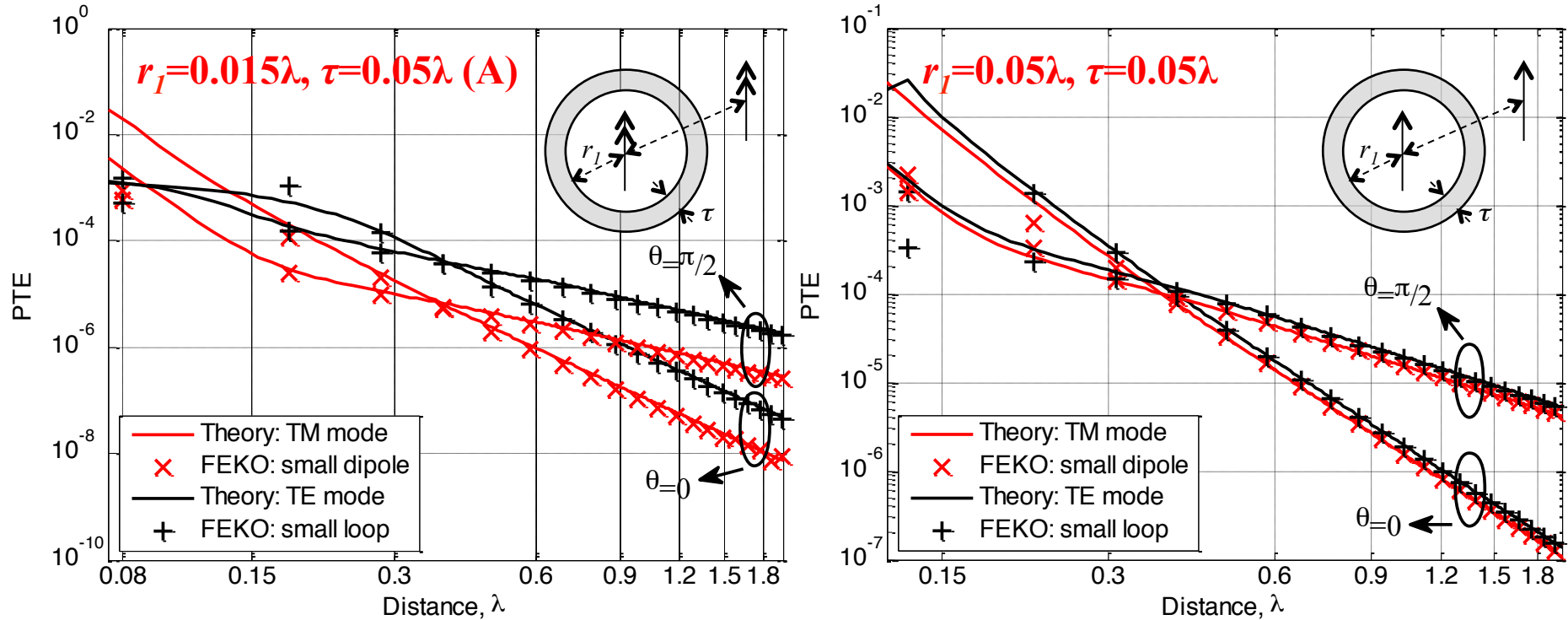
$$PTE_{shell:TM} = \frac{\operatorname{Re}\left[j\hat{H}_1^{(2)'}(k_o r) \cdot \hat{H}_1^{(2)*}(k_o r)\right]}{\operatorname{Re}\left[j\left\{\hat{H}_1^{(2)'}(k_o r) + a_{1:TM} \cdot \hat{J}_1'(k_o r)\right\} \cdot \left\{\hat{H}_1^{(2)*}(k_o r) + a_{1:TM}^* \cdot \hat{J}_1^*(k_o r)\right\}\right]} \times \frac{|X_{shell:TM}|^2}{2 - \operatorname{Re}\left[X_{shell:TM}^2\right] + \sqrt{4\left(1 - \operatorname{Re}\left[X_{shell:TM}^2\right]\right) - \operatorname{Im}\left[X_{shell:TM}^2\right]^2}}$$

- By the use of duality, a final close-form expression for TE mode is given by:

$$PTE_{shell:TE} = \frac{\operatorname{Re}\left[j\hat{H}_1^{(2)}(k_o r) \cdot \hat{H}_1^{(2)*'}(k_o r)\right]}{\operatorname{Re}\left[j\left\{\hat{H}_1^{(2)}(k_o r) + a_{1:TE} \cdot \hat{J}_1(k_o r)\right\} \cdot \left\{\hat{H}_1^{(2)*'}(k_o r) + a_{1:TE}^* \cdot \hat{J}_1^*(k_o r)\right\}\right]} \times \frac{|X_{shell:TE}|^2}{2 - \operatorname{Re}\left[X_{shell:TE}^2\right] + \sqrt{4\left(1 - \operatorname{Re}\left[X_{shell:TE}^2\right]\right) - \operatorname{Im}\left[X_{shell:TE}^2\right]^2}}$$

2. Validation of the theory

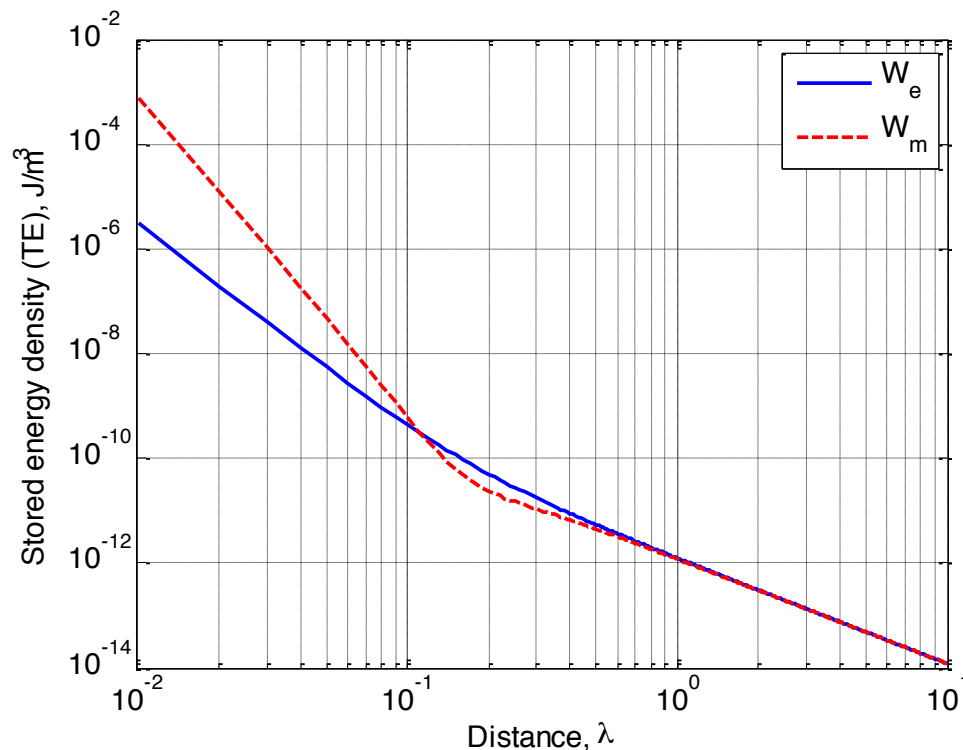
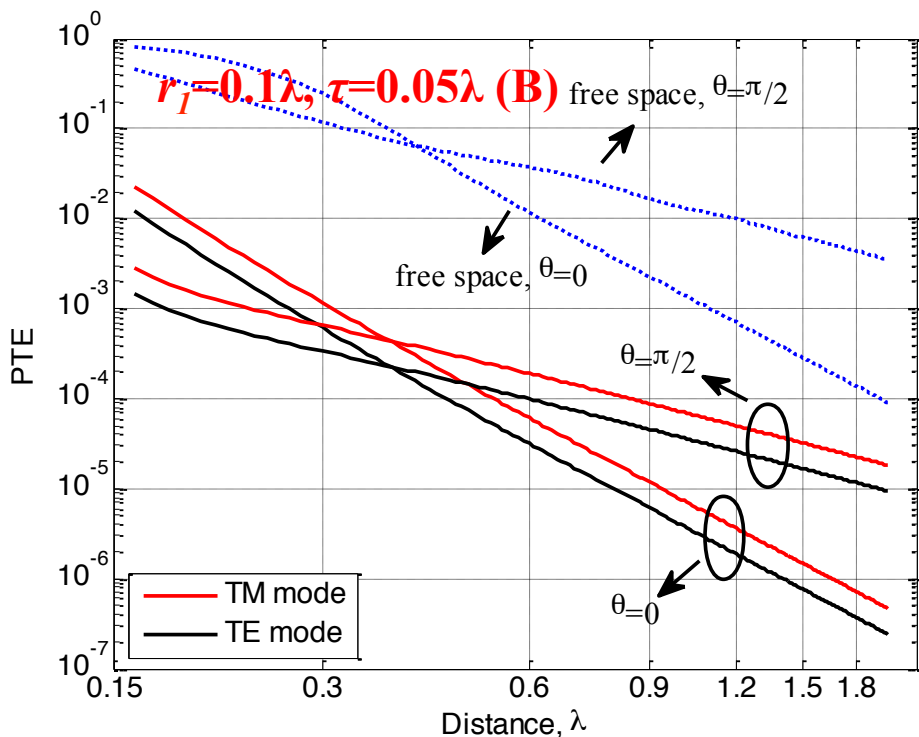
- The derived formulas are compared against numerical simulator, FEKO.
 - Human body fluid is chosen as the material: $\epsilon_r=69.037$, $\tan\delta=1.965$ @200 MHz
 - A $\lambda/50$ -long dipole is used for both the Tx and the Rx for TM mode in FEKO ($\eta_{eff}=1$).
 - A $\lambda/50$ -diameter loop is used for both the Tx and the Rx for TE mode ($\eta_{eff}=1$).
 - The Linville method is utilized to obtain the maximum PTE at each distance.



→ The theory and FEKO show good agreement at distances beyond 0.2λ .

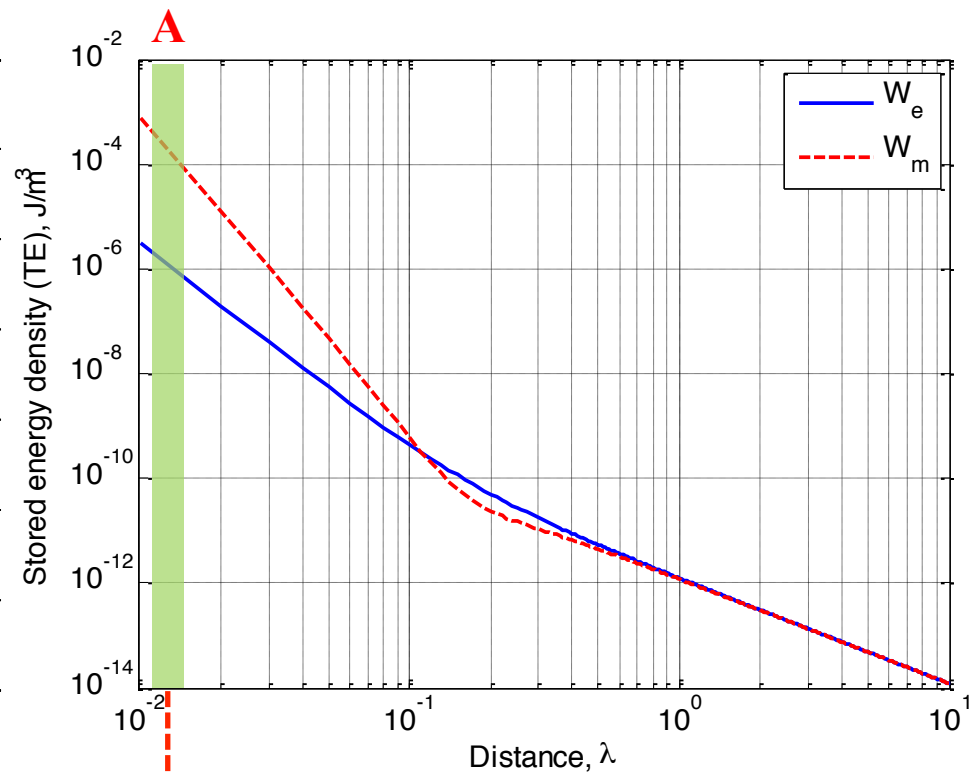
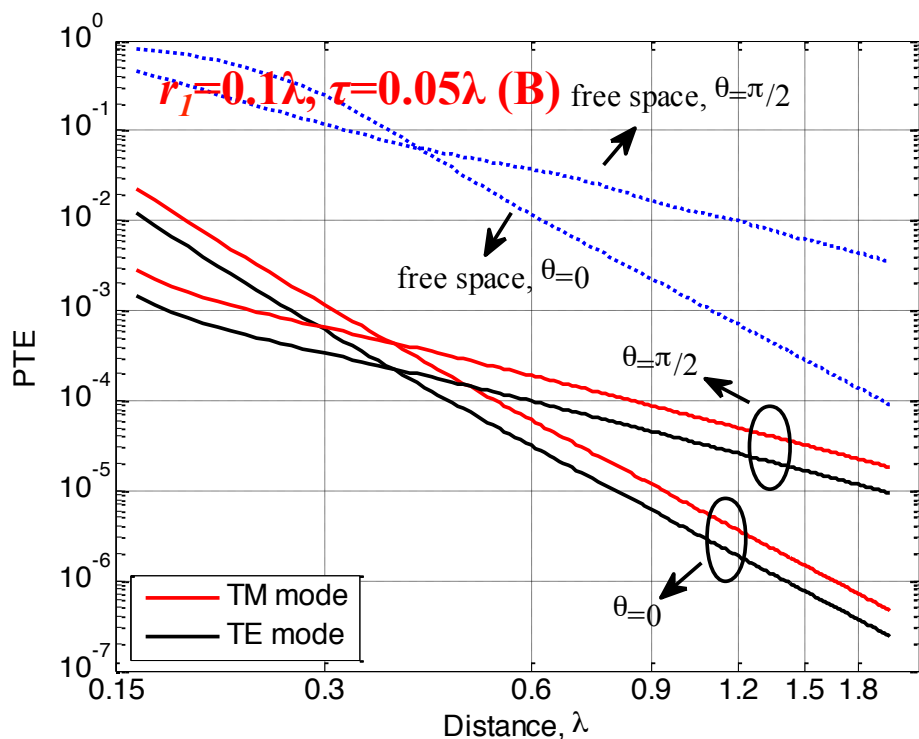
3. PTE under lossy dielectric material

- TM vs. TE modes
 - The shell is filled with the same body fluid material.
 - PTE degradation in comparison to the free space case is shown (due to ϵ_r and $\tan\delta$).
 - TM mode is more efficient than TE mode which is opposite to the previous results.
 - Power transfer using TE mode (i.e. loop) is not strongly affected by dielectric material only when the material is in the extreme near-field region (up to about 0.1λ) of the Tx antenna.



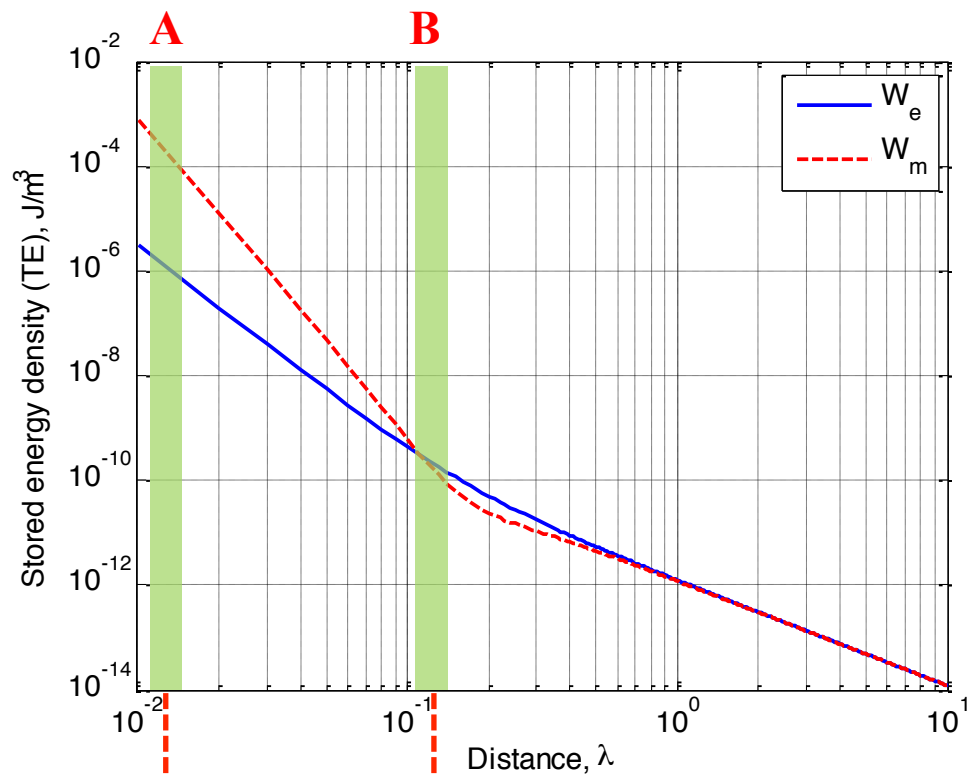
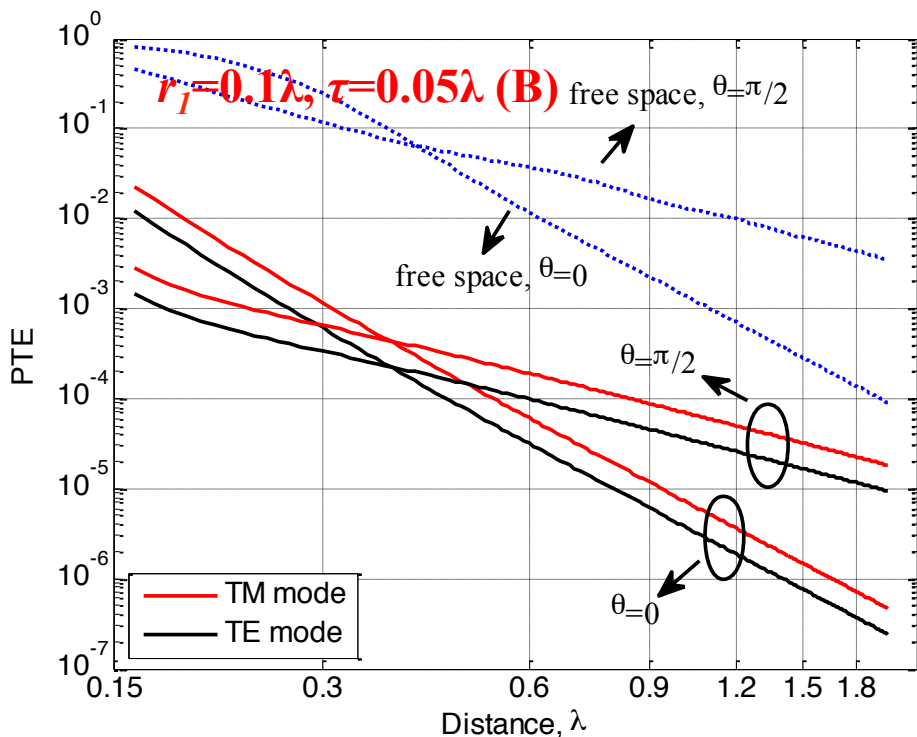
3. PTE under lossy dielectric material

- TM vs. TE modes
 - The shell is filled with the same body fluid material.
 - PTE degradation in comparison to the free space case is shown (due to ϵ_r and $\tan\delta$).
 - TM mode is more efficient than TE mode which is opposite to the previous results.
 - Power transfer using TE mode (i.e. loop) is not strongly affected by dielectric material only when the material is in the extreme near-field region (up to about 0.1λ) of the Tx antenna.



3. PTE under lossy dielectric material

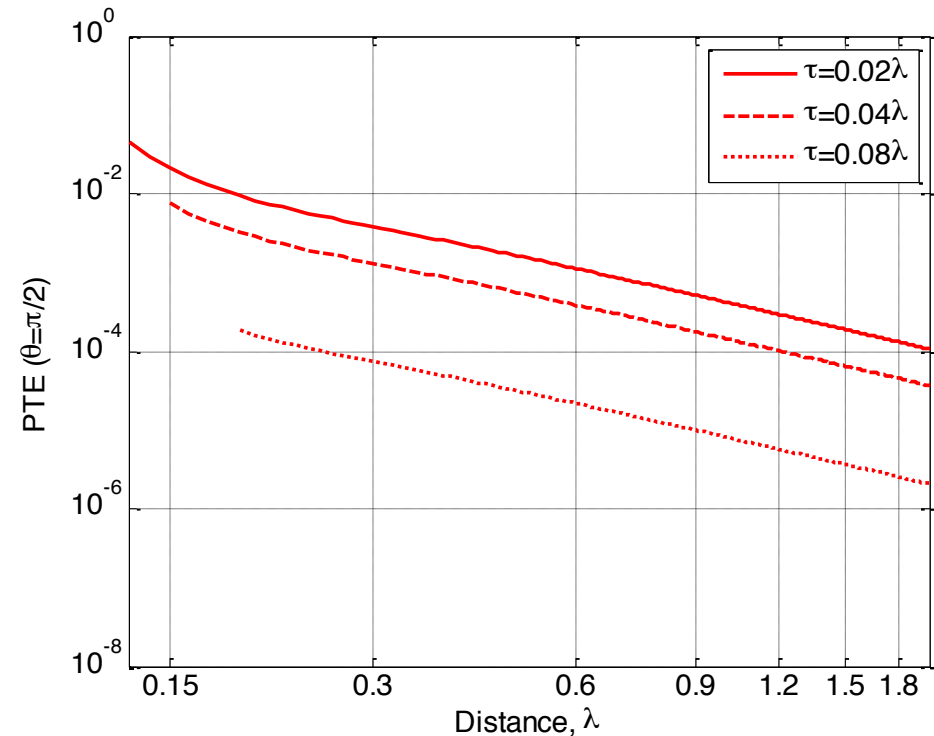
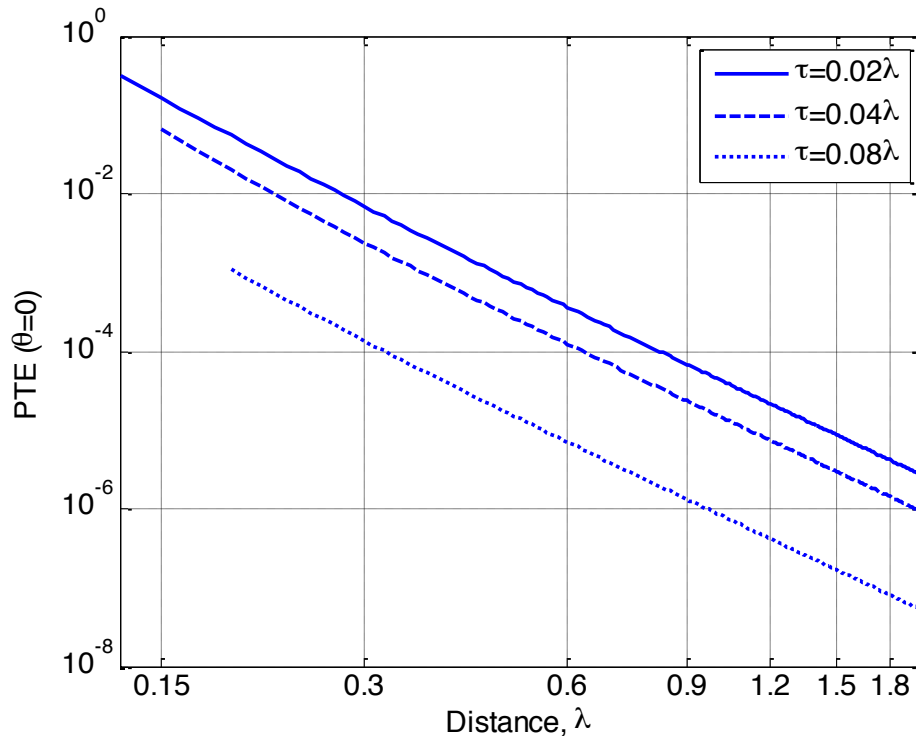
- TM vs. TE modes
 - The shell is filled with the same body fluid material.
 - PTE degradation in comparison to the free space case is shown (due to ϵ_r and $\tan\delta$).
 - TM mode is more efficient than TE mode which is opposite to the previous results.
 - Power transfer using TE mode (i.e. loop) is not strongly affected by dielectric material only when the material is in the extreme near-field region (up to about 0.1λ) of the Tx antenna.



Loop less affected Dipole less affected

■ PTE degradation vs. shell thickness

- Body fluid material.
- r_l is fixed as 0.1λ and τ is changed for both the co-linear and parallel configurations.
- The degradation approximately follows $e^{-2\alpha\tau}$, where α is the attenuation constant inside the shell due to the non-zero loss tangent.

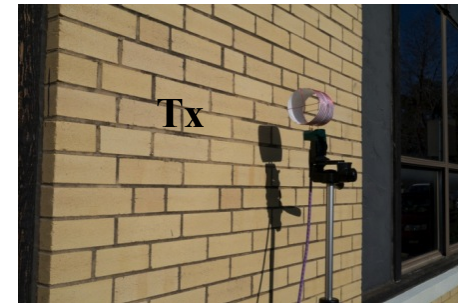
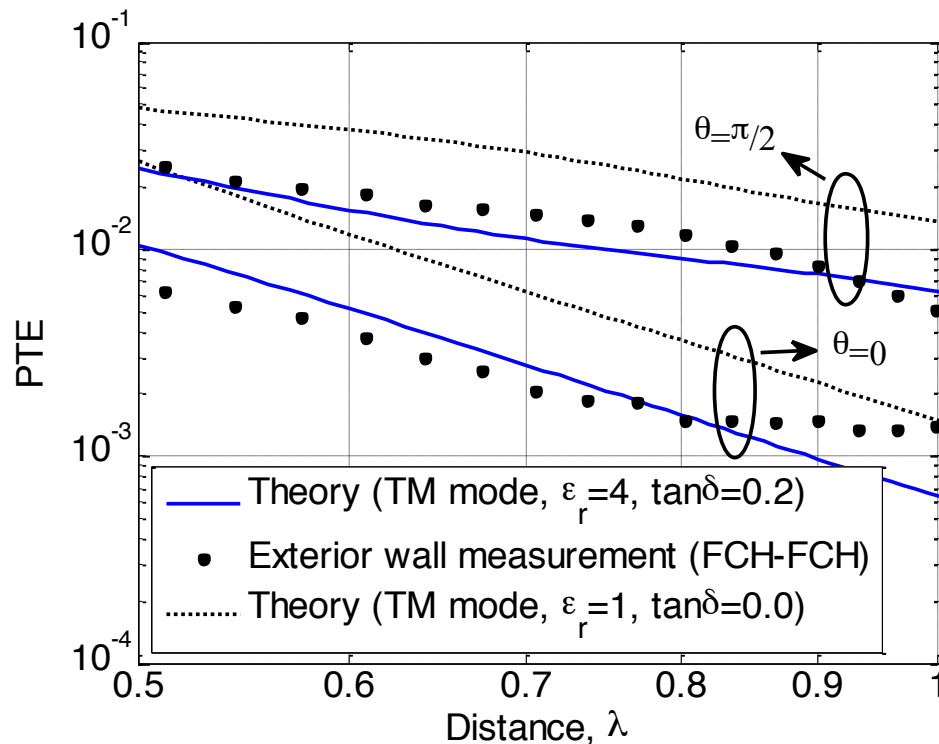


4. Through-wall measurement

- WPT measurements are carried out through walls to examine the effect of materials on the PTE and to corroborate the theory.
 - Even though the measurement geometry is for a planar wall while the theory is derived based on a spherical shell, such comparison may provide an assessment on the predictive value of the derived theoretical bound.
 - Two types of walls are tested: a 37.5cm-thick exterior brick wall and a 13cm-thick interior wall made of wood panel and sheetrock.
 - FCH dipoles, which were used for free space measurement are used. The Tx FCH is fixed at 15cm (0.1λ) from one side of the wall and the Rx FCH is placed at different distances on the other side of the wall.
 - $PTE = |S_{21}|^2 / (1 - |S_{11}|^2)$.

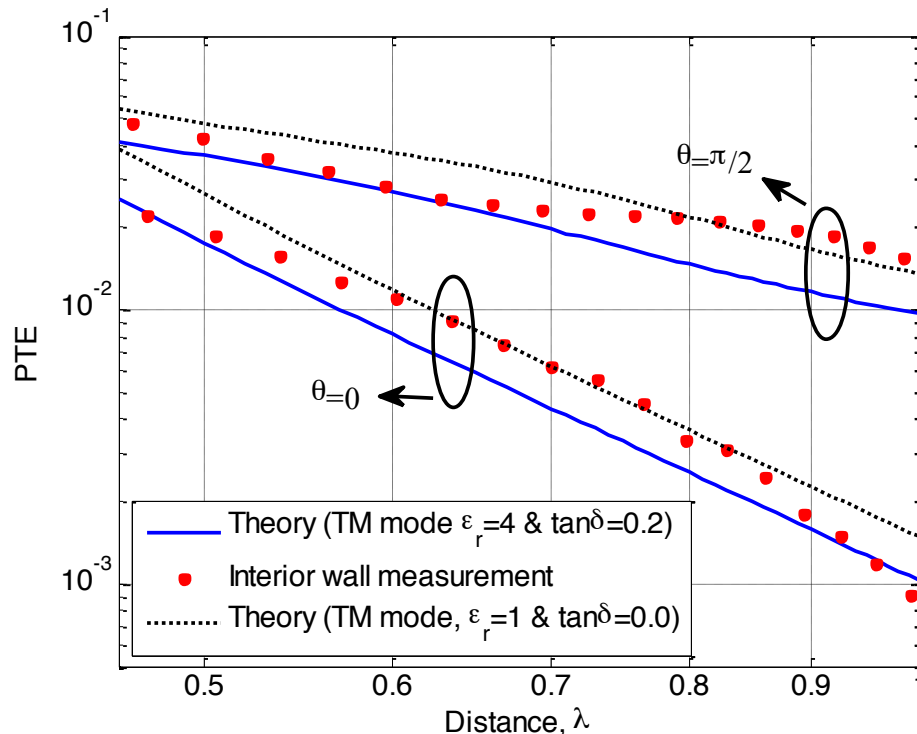
Exterior wall measurement result

- Wall material: $\epsilon_r=4$, $\tan\delta=0.2$ @200MHz ($r_I=0.1\lambda$ and $\tau=0.25\lambda$)
- The measured results (\bullet) are degraded from the free space bound (.....) and approximately follow the theoretical bounds of the material shell (—).



■ Interior wall measurement result

- The same wall material with $r_l=0.15\lambda$ and $\tau=0.1\lambda$.
- It is observed that the measurement results falls approximately between the theoretical PTE values for free space and the assumed $\epsilon_r=4$, $\tan\delta=0.2$ material.
- These through-wall measurement results show the approximate predictive value of the derived theoretical bounds.



- An analytic upper bound for near-field wireless power transfer between a pair of antennas separated by a spherical material shell has been derived.
 - For both TM and TE mode radiators

- The derived closed form expressions have been verified using numerical simulation via FEKO.

- Material effects on wireless power transfer have been studied using the derived closed form expression.
 - TM and TE mode behaviors in power transfer

- Through-wall measurement and comparison with the theory.

I.-J. Yoon and H. Ling, “Investigation of near-field wireless power transfer in the presence of lossy dielectric materials,” *IEEE Trans. Antennas Propag.*, vol. 61 no. 1, pp. 482–488, 2013.



Conclusion

- Demonstrated the theoretical bound can be achieved using actual design of electrically small antennas (Objective 1)

- Enhanced the efficiency of near-field wireless power transfer
 - Transmitter diversity; receiver diversity (Objective 2)
 - Using small directive antennas in near-field region (Objective 4 – not presented today)

- Investigated deployment issues in near-field power transfer
 - Derived theoretical bounds for material effects (Objective 3)
 - Alleviation of polarization mismatch using circular polarization antennas (Objective 5 – not presented today)

- Demonstrated the theoretical bound can be achieved using actual design of electrically small antennas (Objective 1)
- Enhanced the efficiency of near-field wireless power transfer
 - Transmitter diversity; receiver diversity (Objective 2)
 - Using small directive antennas in near-field region (Objective 4 – not presented today)
- Investigated deployment issues in near-field power transfer
 - Derived theoretical bounds for material effects (Objective 3)
 - Alleviation of polarization mismatch using circular polarization antennas (Objective 5 – not presented today)

Near-field region can be used for efficient wireless power transfer.